

Machine learning systems are often deployed for making critical decisions like credit lending, hiring, etc. While making decisions, such systems often encode the user’s demographic information (like gender, age) in their intermediate representations. This can lead to decisions that are biased towards specific demographics. Prior work has focused on debiasing intermediate representations to ensure fair decisions. However, these approaches fail to remain fair with changes in the task or demographic distribution. To ensure fairness in the wild, it is important for a system to adapt to such changes as it accesses new tasks in an incremental fashion. In this work, we propose to address this issue by introducing the problem of learning fair representations in an incremental learning setting. To this end, we present **Fairness-aware Incremental Representation Learning (FaIRL)**, a representation learning system that can sustain fairness while incrementally learning new tasks. FaIRL is able to achieve fairness and learn new tasks by controlling the rate-distortion function of the learned representations. Our empirical evaluations show that FaIRL is able to make fair decisions while achieving high performance on the target task, outperforming several baselines.¹

An increasing number of organizations are leveraging machine learning solutions for making decisions in critical applications like hiring (Dastin, 2018), criminal recidivism (Larson et al., 2016), etc. Machine learning systems can often rely on a user’s demographic information, like gender, race, and age (*protected attributes*), encoded in their representations (Elazar and Goldberg, 2018)

The diagram illustrates an incremental learning system for fair decisions across three tasks. At the top, three cylinders represent 'Task 1', 'Task 2', and 'Task 3'. Arrows point from each task to a corresponding 'Incremental Learning System' (ILS) icon, which is a stylized face with a brain. A dashed arrow connects the ILS icons from left to right, indicating a sequential learning process. Below each ILS is a 'Test' diamond. For Task 1, the test uses only 'Task 1' data. For Task 2, the test uses 'Task 1' and 'Task 2' data. For Task 3, the test uses 'Task 1', 'Task 2', and 'Task 3' data. Each test diamond is connected to a balance scale icon, representing the goal of 'Fair decisions'.

to make decisions, resulting in biased outcomes against certain demographic groups (Mehrabi et al., 2019; Shah, Schwartz, and Hovy, 2020). Numerous works try to achieve fairness through unawareness (Apfelbaum et al., 2010) by debiasing model representations from protected attributes (Blodgett, Green, and O’Connor, 2016; Elazar and Goldberg, 2018; Elazar et al., 2021; Chowdhury and Chaturvedi, 2022). However, these techniques are only able to remove in-domain spurious correlations and fail to generalize to new data distributions (Barrett et al., 2019). For example, let us consider a fair resume screening system that was trained only on resumes of software engineering roles. The system may not remain fair while screening for roles like sales or marketing, where the gender demographic distribution may be different. Similarly, a fair system also needs to be robust to shifts in data distribution (e.g. new applicants may report scores on specific tests that didn’t appear in the training data) and task changes (e.g. resumes being screened for new roles like social media manager). In such cases, it is not always practical to retrain the system from scratch every time new data comes in because of the resources and environmental impact associated with training modern machine learning systems.

Prior works focused on developing robust fair learning models by considering shifts in data distribution. For example, learning fair models under covariate shift (Rezaei et al., 2021; Singh et al., 2021) or for streaming data (Zhang et al., 2021; Zhang and Ntoutsis, 2019), but these systems do not incrementally learn new tasks. In this work, we introduce the problem of *learning fair representations in an incremental learning setting*. In this setting, data from new tasks, with different underlying demographic distributions, pour in at consecutive training stages and the system has to perform well on the new as well as old tasks while making fair decisions (see Figure 1). This is similar to incremental learning (Rebuffi et al., 2017) but most works in incremental learning literature focus on performing well on the target task without considering the fairness of the predictions.

To address this problem, we propose a representation learning system – **Fairness-aware Incremental Representation Learning (FaIRL)**. At its core, FaIRL uses an adversarial debiasing setup for removing demographic information by controlling the number of bits (*rate-distortion*) required to encode the learned representations (Yu et al., 2020; Ma et al., 2007). We leverage this debiasing setup for incremental learning using an exemplar-based approach, by retaining a small set of representative samples from previous tasks, to prevent forgetting. Empirical evaluations show that FaIRL outperforms baseline incremental learning systems in fairness metrics while successfully learning target task information. Our key contributions are:

- We propose FaIRL, a representation learning system that learns fair representations, while incrementally learning new tasks, by controlling their rate-distortion function.
- We show using empirical evaluations that FaIRL outperforms baseline incremental learning systems in making fair decisions while performing well on the target task.
- We also perform extensive analysis experiments to investigate the functioning of FaIRL.

2 Related Work

In this section, we discuss some of the prior works on fairness in varying setups and incremental learning.

Fair Representation Learning. Zemel et al. (2013) introduced the problem of learning fair

representations as an optimization task. Following works (Zhang, Lemoine, and Mitchell, 2018; Li, Baldwin, and Cohn, 2018; Elazar and Goldberg, 2018; Chowdhury et al., 2021) leveraged an adversarial framework (Goodfellow et al., 2014) to achieve fairness, where a discriminator tries to extract demographic information from intermediate representations while performing prediction. Different from these, (Bahng et al., 2020) proposed to learn fair representations, without using protected attribute annotation, by making representations uncorrelated with ones retrieved from a biased classifier. However, these techniques require a target task at hand and are often difficult to train (Elazar and Goldberg, 2018). Another line of work introduced by (Bolukbasi et al., 2016), focuses on debiasing representations independent of a target task. These approaches (Ravfogel et al., 2020; Bolukbasi et al., 2016) iteratively identify subspaces that encode protected attribute information, and project vectors onto their corresponding nullspaces. Recently, Chowdhury and Chaturvedi (2022) proposed a debiasing framework that makes representations from same protected attribute class uncorrelated by maximizing their rate-distortion function. Despite showcasing promise in a single domain, these frameworks fail to remain fair for out-of-distribution data (Barrett et al., 2019).

Fairness under distribution shift. Several works (Rezaei et al., 2021; Singh et al., 2021) have investigated the robustness of fair classifiers under covariate shift. These works identify conditions where fairness can be sustained given shifts in data and label distribution. Efficacy of fair classifiers has also been studied in online settings (Zhang et al., 2021; Zhang and Ntoutsis, 2019), where the data distribution continually evolves depending on the input data stream. However, both lines of work consider a fixed task description at initiation and do not learn new tasks while training.

Incremental Learning. Li and Hoiem (2017) introduced the task of incremental learning and proposed a dynamic architecture leveraging a knowledge distillation loss to prevent catastrophic forgetting (McCloskey and Cohen, 1989). Since then, works on incremental learning can be classified into three broad categories: (a) *Regularization-based* approaches (Li and Hoiem, 2017; Kirkpatrick et al., 2017; Zenke, Poole, and Ganguli, 2017; Castro et al., 2018; Chan et al., 2021) use a

penalty measure to ensure model parameters crucial for previous tasks do not change abruptly; (b) *Dynamic architecture-based* approaches (Long et al., 2015; Rusu et al., 2016; Li et al., 2019) introduce new task-specific parameters to prevent interference with parameters from previous tasks. These architectures grow linearly with the number of tasks having a heavy memory footprint; (c) *Exemplar-based* approaches (Rebuffi et al., 2017; Chaudhry et al., 2019a,b; Tong et al., 2022) maintain a small memory of representative samples from previous tasks and replay them to prevent catastrophic forgetting. Our framework FaIRL is similar to that of Tong et al. (2022), as we also control the rate-distortion of learned representations. However, we also consider the fairness of the predictions by ensuring protected information does not get encoded in the representations.

3 Background

In this section, we discuss the fundamental concepts of rate-distortion theory that form the building blocks of our framework, FaIRL.

Rate Distortion. In information theory (Cover, 1999), the compactness of a distribution is measured by their *coding length* – number of bits required to encode it. In lossy data compression, a set of vectors $Z = \{z_1, \dots, z_n\} \in \mathbb{R}^{n \times d}$, sampled from a distribution $P(Z)$, is encoded using a coding scheme, such that the transmitted vectors $\{\hat{z}_i\}_{i=1}^n$ can be recovered up to a distortion ϵ . The minimal number of bits required per vector to encode the sequence Z is defined by the *rate-distortion* function $R(Z, \epsilon)$. The optimal $R(Z, \epsilon)$ for vectors Z sampled from a multivariate Gaussian $\mathcal{N}(0, \Sigma)$ is:

$$R(Z, \epsilon) = \frac{1}{2} \log_2 \det \left(I + \frac{d}{n\epsilon^2} ZZ^T \right) \quad (1)$$

where n is the number of vectors and d is the dimension of individual vectors. Eq. 1 provides a tight bound even in cases where the underlying distribution $P(Z)$ is degenerate (Ma et al., 2007).

In general scenarios, e.g. image representations for multi-label classification, the vector set Z can arise from a mixture of class distributions. In such cases, the overall rate-distortion function can be computed by splitting the vectors into multiple subsets: $Z = Z^1 \cup Z^2 \dots \cup Z^k$, where Z^j is the subset from the j -th distribution. We can then compute $R(Z^j, \epsilon)$ (Equation 1) for each subset. To facilitate this computation, we leverage a

global membership matrix $\Pi = \{\Pi_j\}_{j=1}^k$, which is a set of k matrices encoding membership information in each subset. The membership matrix for a subset Z^j is a diagonal matrix defined as: $\Pi_j = \text{diag}(\pi_{1j}, \pi_{2j}, \dots, \pi_{nj}) \in \mathbb{R}^{n \times n}$, where $\pi_{ij} \in [0, 1]$ is the probability that z_i belongs to Z^j . The matrices satisfy the following constraints: $\sum_j \Pi_j = I_{n \times n}$, $\sum_j \pi_{ij} = 1$, $\Pi_j \succeq 0$. The optimal number of bits to encode Z is given as:

$$R_c(Z, \epsilon | \Pi) = \sum_{j=1}^k \frac{\text{tr}(\Pi_j)}{2n} \log_2 \det \left(I + \frac{d}{\text{tr}(\Pi_j)\epsilon^2} Z \Pi_j Z^T \right)$$

The expected number of vectors in Z^j is $\text{tr}(\Pi_j)$ and the corresponding covariance is $\frac{1}{\text{tr}(\Pi_j)} Z \Pi_j Z^T$. For multi-class data, a vector z_i can only be a member of a single class, we restrict $\pi_{ij} = \{0, 1\}$ and the covariance matrix for j -th subset is $Z^j (Z^j)^T$.

Maximal Coding Rate (MCR²). Yu et al. (2020) introduced a classification framework by learning discriminative representations using the rate-distortion function. Given n input samples $X = \{x_i\}_{i=1}^n$ belonging to k distinct classes, their representations $Z = \{z_i\}_{i=1}^n$ are obtained using a deep network $f_\theta(x)$. The network parameters (θ) are learned by maximizing a representation-level objective using rate-distortion called maximal coding rate (MCR²):

$$\max_{\theta} \Delta R(Z, \Pi) = R(Z, \epsilon) - R_c(Z, \epsilon | \Pi) \quad (2)$$

where Π captures the class label information. To have discriminative representations, same class representations should resemble each other while being different from representations from other classes. This can be achieved by maximizing the overall volume $R(Z, \epsilon)$ and compressing representations within each class by minimizing $R_c(Z, \epsilon | \Pi)$. We provide further details in Appendix B.

4 Fairness-aware Incremental Representation Learning (FaIRL)

Debiasing Framework

We present a novel adversarial debiasing framework that controls the rate-distortion function of the learned representations. We use rate-distortion

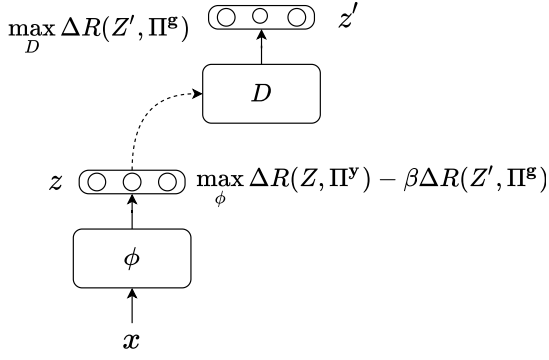


Figure 2: Workflow of our debiasing framework. The discriminator tries to extract protected attribute information by optimizing $\Delta R(Z', \Pi^g)$. The feature encoder tries to learn discriminative representations for the target task (y) using MCR^2 objective while minimizing the discriminator loss.

in this debiasing framework as it is amenable to incremental learning.

Figure 2 illustrates our proposed adversarial framework. It consists of a feature encoder ϕ and a discriminator D . The feature encoder takes as input a data point x and generates representations $z = \phi(x)$. Its goal is to learn representations that are discriminative for the target attribute y and not informative about protected attribute g . The discriminator network takes as input the representations produced by feature encoder z and generates $z' = D(z)$. Its goal is to extract protected attribute g information from z' . The discriminator is trained by maximizing the MCR^2 objective function:

$$\max_D \Delta R(Z', \Pi^g) = R(Z', \epsilon) - R_c(Z', \epsilon | \Pi^g) \quad (3)$$

where Π^g is the membership matrix encoding the protected attribute information. The encoder is trained by optimizing the given objective function:

$$\max_\phi \Delta R(Z, \Pi^y) - \beta \Delta R(Z', \Pi^g) \quad (4)$$

where Π^y is the membership matrix encoding the target attribute information and β is a hyperparameter. Empirically we observed that the proposed debiasing framework is competitive with other debiasing setups in non-incremental learning settings (Section 5).

FaIRL’s debiasing framework leverages the MCR^2 objective (Equation 2) for classification. MCR^2 objective, by itself, is not amenable to incremental learning for reasons discussed below. Yu et al. (2020) showed that using MCR^2

it is possible to learn representations with low-dimensional subspaces corresponding to each class. However, naively maximizing the MCR^2 objective results in representations spanning the complete feature space. This is not ideal for incremental learning as representations from new classes cannot be accommodated in the same feature space. For incremental learning, representations learned at a given training stage should be compact and not span the entire feature space. In FaIRL, we empirically observe that the feature spaces learned at each training stage are compact (Section 5). This happens because while learning discriminative representations using the MCR^2 objective ($\Delta R(Z, \Pi^y)$), the encoder also tries to remove protected information by minimizing $\Delta R(Z', \Pi^g)$ (Equation 4). Minimizing $\Delta R(Z', \Pi^g)$ makes representations from different protected classes similar, resulting in a compact feature space. The $\Delta R(Z', \Pi^g)$ term acts as a natural regularizer to the MCR^2 objective, and prevents the learned representations from expanding in an unconstrained manner, making them suitable for incremental learning. Next, we discuss how to extend this debiasing framework to incremental learning in the following section.

Incremental Learning

For incremental learning, we use an *exemplar-based* approach (Rebuffi et al., 2017; Chaudhry et al., 2019a,b). We store a small set of exemplars from old tasks $\mathcal{X}_{old} = \{\mathcal{X}_{old}^1, \dots, \mathcal{X}_{old}^m\}$, where m is the number of target classes ($m = c(t-1) < k$) the system has encountered so far (each training step introduces c target classes, k is the total number of classes). At training stage t , we have a set of new data samples \mathcal{X}_{new} and exemplar set \mathcal{X}_{old} ($\mathcal{X}_{old} = \emptyset$ at $t = 0$). The goal of our system is to learn discriminative representations w.r.t y for \mathcal{X}_{new} while retaining the old representation subspaces of \mathcal{X}_{old} . To ensure fairness, the system also needs to learn representations that are oblivious to the protected attribute g for both \mathcal{X}_{new} and \mathcal{X}_{old} . We will refer to the representations for the old and new data as $Z_{old} = \phi(\mathcal{X}_{old})$ and $Z_{new} = \phi(\mathcal{X}_{new})$ respectively.

Discriminator. In the incremental learning setup, the discriminator tries to extract protected attribute information for \mathcal{X}_{new} . This is achieved by maximizing $\Delta R(Z'_{new}, \Pi_{new}^g)$, where $Z'_{new} = D(\phi(\mathcal{X}_{new}))$, and Π_{new}^g encodes protected at-

tribute \mathbf{g} information for \mathcal{X}_{new} .

Feature encoder. The goal of the feature encoder is to learn fair representations that are discriminative for both old and new tasks. To achieve this, the system should have the following properties:

1. The system should learn representations for \mathcal{X}_{new} that are informative about \mathbf{y} . This can be achieved by learning discriminative representations for \mathcal{X}_{new} by *maximizing* the MCR² objective: $\Delta R(Z_{new}, \Pi_{new}^{\mathbf{y}})$.
2. The system should not reveal protected information and learn fair representations for \mathcal{X}_{new} . This is achieved by *minimizing* the discriminator loss $\Delta R(Z'_{new}, \Pi_{new}^{\mathbf{g}})$ (Equation 4).
3. The system should retain knowledge about old tasks encountered in previous training stages. FaIRL maintains an exemplar set \mathcal{X}_{old} and tries to retain the subspace structure learned for these samples. To ensure that encoder ϕ_t at training stage t retains the subspace structure of old representations, we *minimize* the function:

$$\begin{aligned} \Delta R(Z_{old}, \bar{Z}_{old}) &= \sum_{i=1}^m \Delta R(Z_{old}^i, \bar{Z}_{old}^i) \\ &= \sum_{i=1}^m R(Z_{old}^i \cup \bar{Z}_{old}^i) - \frac{1}{2} [R(Z_{old}^i) + R(\bar{Z}_{old}^i)] \end{aligned}$$

where $\bar{Z}_{old} = \phi_{t-1}(\mathcal{X}_{old})$ are exemplar representations obtained using the encoder at the previous stage ($t - 1$), and Z_{old}^j are exemplar representations from the j -th target class. $\Delta R(Z_{old}^j, \bar{Z}_{old}^j)$ measures the similarity between the representation sets Z_{old}^j and \bar{Z}_{old}^j by computing the difference in the number of bits required to encode them jointly and separately.

4. The system should learn fair representations for \mathcal{X}_{old} . This is achieved by *minimizing* the discriminator loss for the exemplars $\Delta R(Z'_{old}, \Pi_{old}^{\mathbf{g}})$ (Equation 4).

The overall objective function that the encoder optimizes in the incremental learning setup:

$$\begin{aligned} \max_{\phi} & \underbrace{\Delta R(Z_{new}, \Pi_{new}^{\mathbf{y}})}_{(a)} - \beta \underbrace{\Delta R(Z'_{new}, \Pi_{new}^{\mathbf{g}})}_{(b)} \\ & - \gamma \underbrace{\Delta R(Z_{old}, \bar{Z}_{old})}_{(c)} - \eta \underbrace{\Delta R(Z'_{old}, \Pi_{old}^{\mathbf{g}})}_{(d)} \end{aligned}$$

where $Z'_{old} = D(Z_{old})$, $\Pi_{new}^{\mathbf{y}}$ is the membership matrix encoding target class labels for \mathcal{X}_{new} , $\Pi_{new}^{\mathbf{g}}$

Algorithm 1: Prototype Sampling

```

1: Input:  $Z_t = \{\phi(\mathcal{X}_t^1), \dots, \phi(\mathcal{X}_t^c)\}$  representations of  $c$  classes at training stage  $t$ , reservoir of old samples  $\mathcal{X}_{old}$ .
2:  $\mathcal{X}_{old}^t = \emptyset$   $\triangleright$  exemplars for training stage  $t$ 
3: for  $i = 1, \dots, c$  do
4:    $V^i = \text{PCA}(Z_t^i)$   $\triangleright$  where  $Z_t^i = \mathcal{X}_t^i$ 
5:    $V_k^i = [v_1, \dots, v_k] \sim \text{top-}k(V^i)$   $\triangleright k$  eigen vectors selected based on singular values
6:   for  $j = 1, \dots, r$  do
7:      $s = v_j^T Z_t^i$   $\triangleright$  similarity scores
8:      $\mathcal{X}_{old}^i \sim \text{top-}q(\mathcal{X}_t^i)$   $\triangleright$  select top  $q = \frac{r}{k}$  samples based on similarity scores  $s$ 
9:      $\mathcal{X}_{old}^t = \mathcal{X}_{old}^t \cup \mathcal{X}_{old}^i$ 
10:  end for
11: end for
12:  $\mathcal{X}_{old} = \mathcal{X}_{old} \cup \mathcal{X}_{old}^t$   $\triangleright$  add to exemplar set
13: return  $\mathcal{X}_{old}$ 

```

and $\Pi_{old}^{\mathbf{g}}$ encode protected class labels for \mathcal{X}_{new} and \mathcal{X}_{old} respectively. In the following section, we discuss the selection of representative samples from old classes \mathcal{X}_{old} .

Exemplar Sample Selection

As discussed in previous section, we maintain exemplars $\mathcal{X}_{old} = \{\mathcal{X}_{old}^1, \dots, \mathcal{X}_{old}^m\}$ belonging to m classes, which is useful for retaining information from previous tasks. For each class, we select r (where $r \ll |\mathcal{X}^i|$) samples $\mathcal{X}_{old}^i \sim \mathcal{X}^i$ by using one of the following sampling techniques:

Random Sampling. We randomly select r samples from each class set $\mathcal{X}_{old}^i \sim \mathcal{X}^i$.

Prototype Sampling. We use prototype sampling (Tong et al., 2022) for selecting representative samples for each class. The detailed pseudo-code is presented in Algorithm 1. In this technique, we compute the top k eigenvectors for the set of representations for each class $Z_t^i = \phi(\mathcal{X}_t^i)$ at training stage t . For each eigenvector, we select r/k data samples (\mathcal{X}_{old}^t) with the highest similarity scores (line 7). The selected samples are added to \mathcal{X}_{old} .

Submodular Optimization. We use submodular optimization (Krause and Golovin, 2014) to select representative samples that summarize features of a set. Submodular optimization focuses on set functions which have the diminishing return property. Formally, a submodular function f satisfies the property: $f(Z \cup \{s\}) - f(Z) \geq f(Y \cup \{s\}) - f(Y)$, where $Z \subseteq Y \subseteq S$, $s \in S$, and $s \notin Y$.

We construct a submodular function computed using representations Z that capture their diversity. We select r samples that maximizes f . Specifically, we use the facility location algorithm (Frieze, 1974), which selects r representative samples from a set Z with n elements ($n > r$). For any subset $S \subseteq Z$, the submodular function f is: $f(S) = \sum_{z \in Z} \max_{s \in S} \text{sim}(s, z)$, where $\text{sim}(\cdot, \cdot)$ is the similarity measure between s and z . In our experiments, Z is the set of data representations and we use euclidean distance as our similarity measure $\text{sim}(s, z) = -\|s - z\|_2^2$.

5 Evaluation

In this section, we discuss the datasets, experimental setup, and metrics used for evaluating FaIRL. More details of our experimental setup is reported in Appendix B.

Datasets

We tackle the problem of fairness in an incremental learning setup, where there are no existing benchmarks.² We perform evaluations by repurposing existing datasets.

Biased MNIST. We follow the setup of (Bahng et al., 2020) to generate a synthetic dataset using MNIST (LeCun et al., 1998), by making the background colors highly correlated with the digits. In the training set, the digit category (*target attribute*) is associated with a distinct background color (*protected attribute*) with probability p or a randomly chosen color with probability $1 - p$. In the test set, each digit with assigned one of the 10 colors randomly. We evaluate the generalization ability of FaIRL for $p = \{0.8, 0.85, 0.9, 0.95\}$. We simulate incremental learning by providing the system access to 2 classes at each training stage (a total of 5 stages).



Figure 3: Samples from Biased MNIST dataset.

Biography classification. We re-purpose the BIOS dataset (De-Arteaga et al., 2019) for incremental learning. BIOS contains biographies of

²Most fairness datasets have target attributes with only 2 classes (along with a binary protected attribute), making them unsuitable for evaluating incremental learning.

people that are associated with a profession (*target attribute*) and gender label (*protected attribute*). There are 28 different profession categories and 2 gender classes. The demographic distribution can vary vastly depending on the profession (e.g. ‘software engineer’ role is skewed towards men while the ‘yoga teacher’ role is most associated with females). The detailed demographic distribution is reported in Appendix. In our setup, the system is presented with samples from 5 classes at each training stage (a total of 6 training stages).

Baselines

We compare FaIRL with the following systems:

- **Incremental Learning systems.** We report the performance of the following incremental systems: (a) LwF (Li and Hoiem, 2017) is a dynamic architecture with shared and task specific parameters, with new parameters being added incrementally for new tasks. LwF uses a knowledge distillation loss along with the current task loss to prevent catastrophic forgetting; (b) Adversarial LwF – we introduced an adversarial head in LwF for fair incremental learning that tries to remove protected attribute information via gradient reversal; (c) iCaRL (Rebuffi et al., 2017) is an exemplar-based approach that uses a knowledge distillation loss to learn representations. iCaRL uses a nearest class mean classifier for performing prediction.

- **Joint learning systems.** We report the performance of the following joint learning systems, where the system has access to the entire dataset in a single training stage: (a) AdS (Chowdhury et al., 2021) is an adversarial debiasing framework that maximizes the entropy of discriminator output. (b) FaRM (Chowdhury and Chaturvedi, 2022) is a state-of-the-art system for both constrained and unconstrained debiasing, which performs debiasing by controlling the rate-distortion function of representations; (c) FaIRL (joint). We report the performance of our framework when trained on the entire dataset at once.

Metrics

In this section, we discuss the metrics reported. For each metric, we report the average and the value achieved at the final training stage.

- **Target Accuracy.** We follow (Elazar and Goldberg, 2018; Ravfogel et al., 2020; Chowdhury et al., 2021) in evaluating the quality of the learned representations for target task (\mathbf{y}) by using a separate probing network.

Method	$p = 0.8$		$p = 0.85$		$p = 0.9$		$p = 0.95$	
	Last	Avg.	Last	Avg.	Last	Avg.	Last	Avg.
Incremental	LwF (Li and Hoiem, 2017)	10.28 32.39	10.28 31.50	10.60 31.34	10.28 27.13	10.28 25.79	10.28 25.79	10.28 25.79
	Adversarial LwF	10.28 32.38	10.28 31.94	10.28 27.13	10.28 27.13	10.28 25.79	10.28 25.79	10.28 25.79
	iCaRL (Rebuffi et al., 2017)	62.81 79.20	58.44 72.41	51.08 70.82	47.48 69.86	47.48 69.86	47.48 69.86	47.48 69.86
	FaIRL (random)	81.67 90.44	77.76 88.21	71.05 83.89	59.26 75.66	59.26 75.66	59.26 75.66	59.26 75.66
Joint	FaIRL (prototype)	80.73 89.82	77.18 87.69	70.95 83.47	57.79 75.28	57.79 75.28	57.79 75.28	57.79 75.28
	FaIRL (submod)	80.52 89.84	77.62 88.01	72.24 84.38	57.94 73.48	57.94 73.48	57.94 73.48	57.94 73.48
	FaIRL (joint)	88.08 -	85.64 -	81.94 -	68.85 -	68.85 -	68.85 -	68.85 -
Joint	AdS (Chowdhury et al., 2021)	79.98 -	75.39 -	66.46 -	52.49 -	52.49 -	52.49 -	52.49 -
	FaRM (Chowdhury and Chaturvedi, 2022)	92.44 -	90.54 -	82.55 -	57.09 -	57.09 -	57.09 -	57.09 -

Table 1: Evaluation accuracy of incremental and joint learning systems on Biased MNIST dataset. Performance of joint learning systems are reported in gray. FaIRL achieves the best performance among incremental learning baselines. In strongly correlated settings ($p = 0.95$), FaIRL is competitive with joint learning setups.

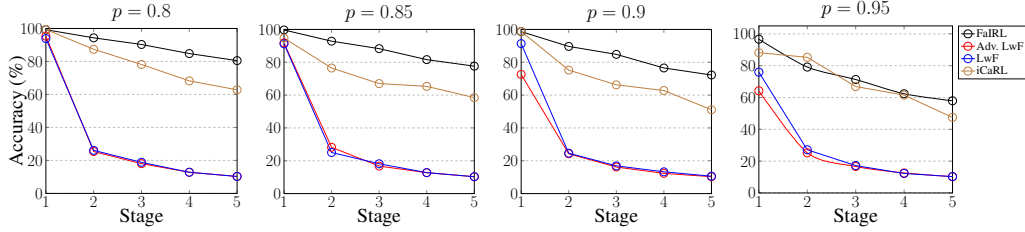


Figure 4: Test accuracy at different training stages of FaIRL and baseline incremental learning systems on Biased MNIST dataset. FaIRL outperforms baselines in all setups.

For Biased MNIST, a fair system would be able to generalize to the test set, therefore target accuracy helps measure the fairness of the system. A higher accuracy is desired in all settings. For both datasets, we also report group fairness metrics discussed below.

• **Group Fairness Metrics.** We evaluate the fairness of representations using the following metrics. A lower score on these metrics indicates a fairer system.

(a) **TPR-GAP.** TPR-GAP (De-Arteaga et al., 2019) computes the difference between true positive rates between two protected groups $\text{Gap}_{\mathbf{g},y} = \text{TPR}_{g,y} - \text{TPR}_{\bar{g},y}$, where g, \bar{g} are possible values of the protected attribute. (Romanov et al., 2019) proposed a single fairness score by computing the root mean square of $\text{Gap}_{\mathbf{g},y}$:

$$\text{Gap}_{\mathbf{g}}^{\text{RMS}} = \sqrt{1/|\mathcal{Y}| \sum_{y \in \mathcal{Y}} (\text{Gap}_{\mathbf{g},y})^2}$$

where \mathcal{Y} is the target label set.

(b) **Demographic Parity (DP).** DP measures the difference in target prediction rate w.r.t. protected

attribute \mathbf{g} . Mathematically, it is expressed as:

$$\text{DP} = \sum_{y \in \mathcal{Y}} |p(\hat{\mathbf{y}} = y | \mathbf{g} = g) - p(\hat{\mathbf{y}} = y | \mathbf{g} = \bar{g})| \quad (5)$$

Zhao and Gordon (2019) illustrated that there is an inherent tradeoff between the utility and fairness in fair representation learning, when \mathbf{y} and \mathbf{g} are correlated. Accordingly, in our experiments, we observe good fairness scores often result in poor target task performance and vice-versa.

Results: Biased MNIST

We report the performance of FaIRL and baselines on Biased MNIST dataset in Table 1. For this dataset, high target accuracy also implies fair decisions as the training sets are biased. We observe that FaIRL outperforms the incremental learning baselines in all settings (different values of p). FaIRL using prototype and submodular exemplar selection approaches slightly fall behind random sampling. We believe that as the class samples are skewed towards a color, these sampling approaches may have ended up selecting instances based on their color instead of the digit infor-

Method		Accuracy (\uparrow)		Fairness			
				DP (\downarrow)		Gap _g ^{RMS} (\downarrow)	
		Last	Avg.			Last	Avg.
Incremental	LwF (Li and Hoiem, 2017)	17.90	52.09	0.25	0.30	0.045	0.015
	Adversarial LwF	21.07	54.21	0.31	0.36	0.185	0.047
	iCaRL (Rebuffi et al., 2017)	97.72	99.08	0.45	0.37	0.095	0.052
	FaIRL (random)	95.11	97.49	0.42	0.35	0.061	0.032
	FaIRL (prototype)	93.93	96.82	0.40	0.34	0.050	0.031
	FaIRL (submodular)	94.37	97.43	0.41	0.35	0.044	0.022
Joint	FaIRL (joint)	98.45	-	0.43	-	0.048	-
	AdS (Chowdhury et al., 2021)	99.90	-	0.45	-	0.003	-
	FaRM (Chowdhury and Chaturvedi, 2022)	99.90	-	0.42	-	0.002	-

Table 2: Target accuracy and fairness metrics achieved by FaIRL and other baselines on Biographies dataset. FaIRL achieves a good balance between target accuracy and fairness metrics.

mation. It is also interesting to note that FaIRL (joint) is competitive with other state-of-the-art approaches AdS and FaRM, outperforming them when the color and digit information are strongly correlated ($p = 0.95$). In this settings ($p = 0.95$), FaIRL even in the incremental learning setting outperforms joint learning baselines. This shows that FaIRL is able to learn robust representations in challenging scenarios where the bias is highly correlated with the target task. We report the fairness metrics in Appendix for completeness.

In Figure 4, we report the performance of incremental learning systems at various training stages. We observe that LwF suffers from catastrophic forgetting, achieving near random performance in the final stages. Adversarial LwF achieves a similar performance to LwF. We believe that the adversarial head doesn’t provide an added advantage over LwF because it may encounter unseen classes of protected attribute (colors) at later training stages. iCaRL and FaIRL do not suffer from catastrophic forgetting, and in all settings FaIRL consistently outperforms other baselines.

Results: Biography Classification

We present the results of FaIRL on Biography classification in Table 2. We observe that LwF-based systems achieve poor target performance due to catastrophic forgetting. However, as most of their predictions are incorrect these systems end up with good scores on fairness metrics. Adversarial LwF performs slightly better than LwF in terms of target accuracy. iCaRL achieves the best target accuracy but performs the worst on fairness metrics. FaIRL provides a good balance between the two traits – achieving target accuracy comparable

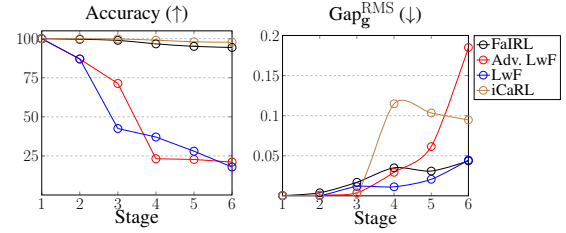


Figure 5: Evolution of target accuracy and Gap_g^{RMS} at different training stages.

to iCaRL while significantly improving the fairness metrics.

We observe that FaIRL (joint) is competitive with state-of-the-art debiasing frameworks AdS and FaRM. It is interesting to note that incrementally trained FaIRL achieves better DP scores than jointly trained debiasing frameworks. We report the target accuracy and Gap_g^{RMS} metric across training stages. In Figure 5(a), FaIRL outperforms most baselines, marginally falling short of iCaRL in the final training stages. However, the Gap_g^{RMS} metric (in Figure 5(b)) for FaIRL is much better than iCaRL. LwF-based systems also achieve low scores but this is because of underfitting as evident from their low target accuracies.

Analysis

In this section, we perform several analysis experiments to investigate the functioning of FaIRL.

Task ablations. We vary the number of classes that FaIRL is presented with at a given training stage and report the average accuracy and fairness scores on Biographies dataset. In Table 3, we observe a significant drop in target performance when the number of classes (in a training stage)

# classes	Acc. (\uparrow)	DP (\downarrow)	Gap _g ^{RMS} (\downarrow)
2	89.47	0.26	0.046
5	97.49	0.35	0.032
10	98.57	0.39	0.031

Table 3: Performance of FaIRL with varying number of classes per training stage.

are reduced accompanied by an improvement in DP, reflecting the tradeoff between fairness and utility as noted by (Zhao and Gordon, 2019). The complete results for all sampling strategies are reported in Appendix C.

Evolution of feature space. We investigate the evolution of $R(Z)$ in FaIRL, which captures the volume of the feature space. In Figure 6(a), we observe that having the debiasing component ($\beta > 0$ in Equation 4) keeps the overall feature space compact (low $R(Z)$ values), which helps in incremental learning. However, a very high value of β can prevent the feature space from expanding at all (shown in Figure 6(a)) thereby resulting in poor target task performance.

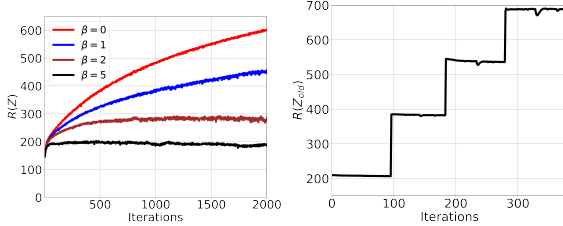


Figure 6: Evolution of $R(Z)$ in FaIRL over different training iterations.

In Figure 6(b), we visualize the rate-distortion of the exemplar samples $R(Z_{old})$ as the training progressed. We observe a sharp rise in $R(Z_{old})$ at certain iterations, where new classes are added at every training stage. This shows that FaIRL is able to leverage its compact feature space to gracefully accommodate representations from new tasks.

Visualization. We visualize the UMAP (McInnes, Healy, and Melville, 2018) feature projections before and after the debiasing process in Biographies dataset. The feature vectors are color-coded according to the protected attribute (gender). In Figure 7, we observe that before training (left) it is easier to distinguish features, and features after training using FaIRL (right) from both gender encompass similar subspaces.

We report additional analysis experiments to in-

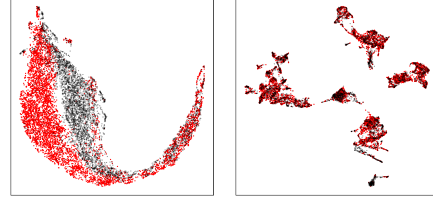


Figure 7: UMAP feature projections before and after incremental learning using FaIRL.

vestigate the memory usage, sample efficiency, robustness, and effect of exemplar size on FaIRL’s performance in Appendix C.

6 Conclusion

In this work, we tackled the problem of learning fair representations in an incremental learning setting. To achieve this, we proposed **F**airness-**a**ware **I**ncremental **R**epresentation **L**earning (FaIRL), a representation learning system that can make fair decisions while learning new tasks by controlling the rate-distortion function of representations. Empirical evaluations show that FaIRL is able to make fair decisions outperforming prior baselines, even in scenarios where the target and protected attributes are strongly correlated. Through extensive analysis, we observe that the debiasing framework at the core of FaIRL is able to keep the feature compact, which helps FaIRL to learn new tasks in an incremental fashion. Our proposed work FaIRL can make fair decisions with incremental access to unseen tasks. Such systems will be crucial for achieving fairness in the wild, as learning systems are increasingly being deployed to critical applications. Future works can focus on developing incrementally trained fair decision-making systems with minimal reliance on protected attribute annotations.

References

- Apfelbaum, E. P.; Pauker, K.; Sommers, S. R.; and Ambady, N. 2010. In blind pursuit of racial equality? *Psychological science*, 21(11): 1587–1592.
- Bahng, H.; Chun, S.; Yun, S.; Choo, J.; and Oh, S. J. 2020. Learning De-biased Representations with Biased Representations. In *Proceedings of the 37th International Conference on Machine Learning, ICML 2020, 13-18 July 2020, Virtual*

- Event, volume 119 of *Proceedings of Machine Learning Research*, 528–539. PMLR.
- Barrett, M.; Kementchedjieva, Y.; Elazar, Y.; Elliott, D.; and Søgaard, A. 2019. Adversarial Removal of Demographic Attributes Revisited. In *Proceedings of the 2019 Conference on Empirical Methods in Natural Language Processing and the 9th International Joint Conference on Natural Language Processing (EMNLP-IJCNLP)*, 6330–6335. Hong Kong, China: Association for Computational Linguistics.
- Blodgett, S. L.; Green, L.; and O’Connor, B. 2016. Demographic Dialectal Variation in Social Media: A Case Study of African-American English. In *Proceedings of the 2016 Conference on Empirical Methods in Natural Language Processing*, 1119–1130. Austin, Texas: Association for Computational Linguistics.
- Bolukbasi, T.; Chang, K.; Zou, J. Y.; Saligrama, V.; and Kalai, A. T. 2016. Man is to Computer Programmer as Woman is to Homemaker? Debiasing Word Embeddings. In Lee, D. D.; Sugiyama, M.; von Luxburg, U.; Guyon, I.; and Garnett, R., eds., *Advances in Neural Information Processing Systems 29: Annual Conference on Neural Information Processing Systems 2016, December 5-10, 2016, Barcelona, Spain*, 4349–4357.
- Castro, F. M.; Marín-Jiménez, M. J.; Guil, N.; Schmid, C.; and Alahari, K. 2018. End-to-end incremental learning. In *Proceedings of the European conference on computer vision (ECCV)*, 233–248.
- Chan, K. H. R.; Yu, Y.; You, C.; Qi, H.; Wright, J.; and Ma, Y. 2021. ReduNet: A white-box deep network from the principle of maximizing rate reduction. *ArXiv preprint*, abs/2105.10446.
- Chaudhry, A.; Ranzato, M.; Rohrbach, M.; and Elhoseiny, M. 2019a. Efficient Lifelong Learning with A-GEM. In *7th International Conference on Learning Representations, ICLR 2019, New Orleans, LA, USA, May 6-9, 2019*. OpenReview.net.
- Chaudhry, A.; Rohrbach, M.; Elhoseiny, M.; Ajanthan, T.; Dokania, P. K.; Torr, P. H.; and Ranzato, M. 2019b. On tiny episodic memories in continual learning. *ArXiv preprint*, abs/1902.10486.
- Chowdhury, S.; Ghosh, S.; Li, Y.; Oliva, J.; Srivastava, S.; and Chaturvedi, S. 2021. Adversarial Scrubbing of Demographic Information for Text Classification. In *Proceedings of the 2021 Conference on Empirical Methods in Natural Language Processing*, 550–562. Online and Punta Cana, Dominican Republic: Association for Computational Linguistics.
- Chowdhury, S. B. R.; and Chaturvedi, S. 2022. Learning Fair Representations via Rate-Distortion Maximization. *ArXiv preprint*, abs/2202.00035.
- Cover, T. M. 1999. *Elements of information theory*. John Wiley & Sons.
- Dastin, J. 2018. Amazon scraps secret AI recruiting tool that showed bias against women. In *Ethics of Data and Analytics*, 296–299. Auerbach Publications.
- De-Arteaga, M.; Romanov, A.; Wallach, H.; Chayes, J.; Borgs, C.; Chouldechova, A.; Geyik, S.; Kenthapadi, K.; and Kalai, A. T. 2019. Bias in bios: A case study of semantic representation bias in a high-stakes setting. In *proceedings of the Conference on Fairness, Accountability, and Transparency*, 120–128.
- Elazar, Y.; and Goldberg, Y. 2018. Adversarial Removal of Demographic Attributes from Text Data. In *Proceedings of the 2018 Conference on Empirical Methods in Natural Language Processing*, 11–21. Brussels, Belgium: Association for Computational Linguistics.
- Elazar, Y.; Ravfogel, S.; Jacovi, A.; and Goldberg, Y. 2021. Amnesic probing: Behavioral explanation with amnesic counterfactuals. *Transactions of the Association for Computational Linguistics*, 9: 160–175.
- Frieze, A. M. 1974. A cost function property for plant location problems. *Mathematical Programming*, 7(1): 245–248.
- Goodfellow, I. J.; Pouget-Abadie, J.; Mirza, M.; Xu, B.; Warde-Farley, D.; Ozair, S.; Courville, A.; and Bengio, Y. 2014. Generative adversarial networks. *ArXiv preprint*, abs/1406.2661.

- Kirkpatrick, J.; Pascanu, R.; Rabinowitz, N.; Veness, J.; Desjardins, G.; Rusu, A. A.; Milan, K.; Quan, J.; Ramalho, T.; Grabska-Barwinska, A.; et al. 2017. Overcoming catastrophic forgetting in neural networks. *Proceedings of the national academy of sciences*, 114(13): 3521–3526.
- Krause, A.; and Golovin, D. 2014. Submodular function maximization. *Tractability*, 3: 71–104.
- Larson, J.; Mattu, S.; Kirchner, L.; and Angwin, J. 2016. How we analyzed the COMPAS recidivism algorithm. *ProPublica (5 2016)*, 9(1): 3–3.
- LeCun, Y.; Bottou, L.; Bengio, Y.; and Haffner, P. 1998. Gradient-based learning applied to document recognition. *Proceedings of the IEEE*, 86(11): 2278–2324.
- Li, X.; Zhou, Y.; Wu, T.; Socher, R.; and Xiong, C. 2019. Learn to Grow: A Continual Structure Learning Framework for Overcoming Catastrophic Forgetting. In Chaudhuri, K.; and Salakhutdinov, R., eds., *Proceedings of the 36th International Conference on Machine Learning, ICML 2019, 9-15 June 2019, Long Beach, California, USA*, volume 97 of *Proceedings of Machine Learning Research*, 3925–3934. PMLR.
- Li, Y.; Baldwin, T.; and Cohn, T. 2018. Towards Robust and Privacy-preserving Text Representations. In *Proceedings of the 56th Annual Meeting of the Association for Computational Linguistics (Volume 2: Short Papers)*, 25–30. Melbourne, Australia: Association for Computational Linguistics.
- Li, Z.; and Hoiem, D. 2017. Learning without forgetting. *IEEE transactions on pattern analysis and machine intelligence*, 40(12): 2935–2947.
- Long, M.; Cao, Y.; Wang, J.; and Jordan, M. I. 2015. Learning Transferable Features with Deep Adaptation Networks. In Bach, F. R.; and Blei, D. M., eds., *Proceedings of the 32nd International Conference on Machine Learning, ICML 2015, Lille, France, 6-11 July 2015*, volume 37 of *JMLR Workshop and Conference Proceedings*, 97–105. JMLR.org.
- Ma, Y.; Derksen, H.; Hong, W.; and Wright, J. 2007. Segmentation of multivariate mixed data via lossy data coding and compression. *IEEE transactions on pattern analysis and machine intelligence*, 29(9): 1546–1562.
- McCloskey, M.; and Cohen, N. J. 1989. Catastrophic interference in connectionist networks: The sequential learning problem. In *Psychology of learning and motivation*, volume 24, 109–165. Elsevier.
- McInnes, L.; Healy, J.; and Melville, J. 2018. Umap: Uniform manifold approximation and projection for dimension reduction. *ArXiv preprint*, abs/1802.03426.
- Mehrabi, N.; Morstatter, F.; Saxena, N.; Lerman, K.; and Galstyan, A. 2019. A survey on bias and fairness in machine learning. *ArXiv preprint*, abs/1908.09635.
- Paszke, A.; Gross, S.; Massa, F.; Lerer, A.; Bradbury, J.; Chanan, G.; Killeen, T.; Lin, Z.; Gimelshein, N.; Antiga, L.; Desmaison, A.; Köpf, A.; Yang, E.; DeVito, Z.; Raison, M.; Tejani, A.; Chilamkurthy, S.; Steiner, B.; Fang, L.; Bai, J.; and Chintala, S. 2019. PyTorch: An Imperative Style, High-Performance Deep Learning Library. In Wallach, H. M.; Larochelle, H.; Beygelzimer, A.; d’Alché-Buc, F.; Fox, E. B.; and Garnett, R., eds., *Advances in Neural Information Processing Systems 32: Annual Conference on Neural Information Processing Systems 2019, NeurIPS 2019, December 8-14, 2019, Vancouver, BC, Canada*, 8024–8035.
- Ravfogel, S.; Elazar, Y.; Gonen, H.; Twiton, M.; and Goldberg, Y. 2020. Null It Out: Guarding Protected Attributes by Iterative Nullspace Projection. In *Proceedings of the 58th Annual Meeting of the Association for Computational Linguistics*, 7237–7256. Online: Association for Computational Linguistics.
- Rebuffi, S.; Kolesnikov, A.; Sperl, G.; and Lampert, C. H. 2017. iCaRL: Incremental Classifier and Representation Learning. In *2017 IEEE Conference on Computer Vision and Pattern Recognition, CVPR 2017, Honolulu, HI, USA, July 21-26, 2017*, 5533–5542. IEEE Computer Society.
- Rezaei, A.; Liu, A.; Memarrast, O.; and Ziebart, B. D. 2021. Robust fairness under covariate shift. In *Proceedings of the AAAI Conference on Artificial Intelligence*, volume 35, 9419–9427.

- Romanov, A.; De-Arteaga, M.; Wallach, H.; Chayes, J.; Borgs, C.; Chouldechova, A.; Geyik, S.; Kenthapadi, K.; Rumshisky, A.; and Kalai, A. 2019. What’s in a Name? Reducing Bias in Bios without Access to Protected Attributes. In *Proceedings of the 2019 Conference of the North American Chapter of the Association for Computational Linguistics: Human Language Technologies, Volume 1 (Long and Short Papers)*, 4187–4195. Minneapolis, Minnesota: Association for Computational Linguistics.
- Rusu, A. A.; Rabinowitz, N. C.; Desjardins, G.; Soyer, H.; Kirkpatrick, J.; Kavukcuoglu, K.; Pascanu, R.; and Hadsell, R. 2016. Progressive neural networks. *ArXiv preprint*, abs/1606.04671.
- Shah, D. S.; Schwartz, H. A.; and Hovy, D. 2020. Predictive Biases in Natural Language Processing Models: A Conceptual Framework and Overview. In *Proceedings of the 58th Annual Meeting of the Association for Computational Linguistics*, 5248–5264. Online: Association for Computational Linguistics.
- Singh, H.; Singh, R.; Mhasawade, V.; and Churnara, R. 2021. Fairness violations and mitigation under covariate shift. In *Proceedings of the 2021 ACM Conference on Fairness, Accountability, and Transparency*, 3–13.
- Tong, S.; Dai, X.; Wu, Z.; Li, M.; Yi, B.; and Ma, Y. 2022. Incremental Learning of Structured Memory via Closed-Loop Transcription. *ArXiv preprint*, abs/2202.05411.
- Yu, Y.; Chan, K. H. R.; You, C.; Song, C.; and Ma, Y. 2020. Learning diverse and discriminative representations via the principle of maximal coding rate reduction. *ArXiv preprint*, abs/2006.08558.
- Zemel, R. S.; Wu, Y.; Swersky, K.; Pitassi, T.; and Dwork, C. 2013. Learning Fair Representations. In *Proceedings of the 30th International Conference on Machine Learning, ICML 2013, Atlanta, GA, USA, 16-21 June 2013*, volume 28 of *JMLR Workshop and Conference Proceedings*, 325–333. JMLR.org.
- Zenke, F.; Poole, B.; and Ganguli, S. 2017. Continual Learning Through Synaptic Intelligence. In Precup, D.; and Teh, Y. W., eds., *Proceedings of the 34th International Conference on Machine Learning, ICML 2017, Sydney, NSW, Australia, 6-11 August 2017*, volume 70 of *Proceedings of Machine Learning Research*, 3987–3995. PMLR.
- Zhang, B. H.; Lemoine, B.; and Mitchell, M. 2018. Mitigating unwanted biases with adversarial learning. In *Proceedings of the 2018 AAAI/ACM Conference on AI, Ethics, and Society*, 335–340.
- Zhang, W.; Bifet, A.; Zhang, X.; Weiss, J. C.; and Nejd, W. 2021. Farf: A fair and adaptive random forests classifier. In *Pacific-Asia Conference on Knowledge Discovery and Data Mining*, 245–256. Springer.
- Zhang, W.; and Ntoutsis, E. 2019. FAHT: An Adaptive Fairness-aware Decision Tree Classifier. In *IJCAI*.
- Zhao, H.; and Gordon, G. J. 2019. Inherent Trade-offs in Learning Fair Representations. In Wallach, H. M.; Larochelle, H.; Beygelzimer, A.; d’Alché-Buc, F.; Fox, E. B.; and Garnett, R., eds., *Advances in Neural Information Processing Systems 32: Annual Conference on Neural Information Processing Systems 2019, NeurIPS 2019, December 8-14, 2019, Vancouver, BC, Canada*, 15649–15659.

A Appendix

B Method Implementation

MCR² Illustration. We illustrate the implementation of MCR² for multi-label classification using a simple example. Specifically, we focus on the construction of the global membership matrix Π , which is a collection of diagonal matrices $\Pi = \{\Pi_j\}_{j=1}^k$ for each of the k classes. For each class, Π_j is defined as:

$$\Pi_j = \begin{bmatrix} \pi_{1j} & 0 & \dots & 0 \\ 0 & \pi_{2j} & \dots & 0 \\ \vdots & \vdots & \ddots & \vdots \\ 0 & 0 & \dots & \pi_{nj} \end{bmatrix} \in \mathbb{R}^{n \times n} \quad (6)$$

where n is the number of data samples. For multi-label classification, where a data sample can be a member of a single class $\pi_{ij} \in \{0, 1\}$. Let us consider a dataset with 4 samples $Z = \{z_i\}_{i=1}^4$ from 2 distinct classes with labels $y = \{1, 2, 1, 1\}$. The corresponding membership matrices are:

$$\Pi_1 = \begin{bmatrix} 1 & 0 & 0 & 0 \\ 0 & 0 & 0 & 0 \\ 0 & 0 & 1 & 0 \\ 0 & 0 & 0 & 1 \end{bmatrix}, \quad \Pi_2 = \begin{bmatrix} 0 & 0 & 0 & 0 \\ 0 & 1 & 0 & 0 \\ 0 & 0 & 0 & 0 \\ 0 & 0 & 0 & 0 \end{bmatrix} \quad (7)$$

$\Pi = \{\Pi_1, \Pi_2\}$ matrices are used for computing the second term in MCR² ($R_c(Z, \epsilon | \Pi)$ in Equation 2). This process is followed to encode prediction label $y \in \mathbb{R}^n$ information for multi-label classification

Dataset Statistics. We repurpose the original MNIST dataset to generate Biased MNIST. It has 60K training samples, and 10K test samples. The details of the coloring process is discussed in Section 5. Biographies dataset has 257K training samples, 40K dev samples, and 99K test samples. Every biography in this dataset is associated with one of 28 profession categories, and a binary gender label. Biographies contain personally identifiable information that are already available on the internet. De-Arteaga et al. (2019) curated the dataset with appropriate approval and publicly released it for academic usage. We did not perform any additional data collection. The demographic distribution of Biographies dataset is shown in Figure 8. We observe that the gender distribution is skewed for certain professions like surgeon, dietician etc.

Experimental Setup. For Biased MNIST dataset, our feature encoder ϕ is a two-layer CNN network with kernel size 5×5 , followed by a

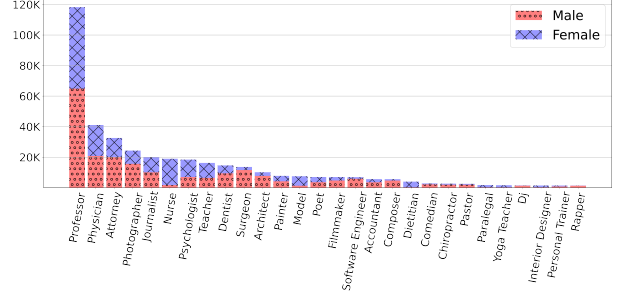


Figure 8: Demographic distribution of different professions in Biographies dataset.

fully-connected network. For Biographies, ϕ is a BERT_{base} encoder followed by a 2-layer MLP. The discriminator is a 2-layer fully connected network. We use the same feature encoder for all setups including the baselines. The model was trained using Adam Optimizer with a learning rate of 2×10^{-5} . All experiments were implemented using PyTorch (Paszke et al., 2019). We trained our model for 2 epochs at each training stages using a single GeForce GTX 2080 Ti GPU. We set $\beta = \gamma = \eta = 1$ for Biographies, and $\beta = \eta = 0.01, \gamma = 1$ for Biased MNIST dataset respectively. All hyperparameters were tuned on the development set of each dataset. Implementation of the baseline approach iCaRL was adapted from the open-sourced project.³ In Biased MNIST dataset, most digit classes have similar number of samples, therefore we present incremental learning systems classes in a random order. In Biographies dataset, we present incremental learning systems with classes in descending order of their size (number of samples in their class). The order of class sequence for Biographies is shown in Figure 8. We provide the system with 5 classes at each training stage (except in the last training stage, where it has access to 3 classes). For both datasets, we select 20 samples per class as the exemplar set. This is quite small compared to the average class sizes in the training set: Biographies $\sim 9.2K$, Biased MNIST $\sim 6K$ samples.

C Additional Analysis

Memory Usage. In this experiment, we report how the GPU memory usage varies during training FaRL. We perform this experiment on Biased MNIST dataset with random sampling strategy and varying exemplar set sizes. In Figure 9, we

³<https://github.com/donlee90/icarl>

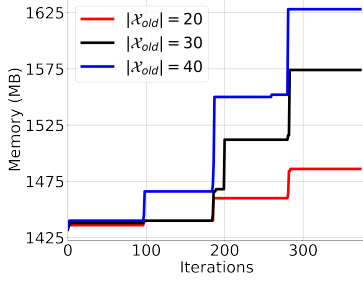


Figure 9: GPU memory usage over training iterations. We observe incremental gain in memory usage over iterations.

observe that memory usage increases over training iterations as exemplar set becomes larger. However, the gain in memory usage at a training step is small ($< 10\%$) compared to the total memory being used. We also observe that the growth in memory usage rises progressively as the exemplar set size increases.

Ablation with number of tasks. We extend the ablation experiments on the number of classes FaIRL receives at each training stage for all sampling strategies. In Table 4, we report the average performance metrics of FaIRL on Biographies dataset using varying sampling strategies. Similar trends noted in Section 5 hold true for all settings. It is interesting to note that when the number of classes=2, prototypical sampling outperforms other strategies by a significant margin in terms of target accuracy.

Sampling	# classes	Acc. (\uparrow)	DP (\downarrow)	Gap _g ^{RMS} (\downarrow)
<i>random</i>	2	89.47	0.26	0.046
	5	97.49	0.35	0.032
	10	98.57	0.39	0.031
<i>prototypical</i>	2	92.12	0.28	0.042
	5	93.93	0.34	0.031
	10	98.33	0.39	0.030
<i>submodular</i>	2	86.29	0.24	0.033
	5	94.37	0.35	0.022
	10	98.48	0.39	0.040

Table 4: Performance of FaIRL with varying number of classes on Biographies dataset.

Effect of the Debiasing Component. In this experiment, we investigate the effect of the debiasing component on incremental learning task. We perform ablations of FaIRL by changing the hyperparameters β, η (Equation 4). In Table 5, we report the amortized accuracy, leakage and fairness

Configuration	Acc. (\uparrow)	Leakage (\downarrow)	DP (\downarrow)	Gap _g ^{RMS} (\downarrow)
$(\beta = 0, \eta = 0)$	91.19	43.28	0.36	0.129
$(\beta = 0, \eta = 1)$	94.78	41.97	0.37	0.094
$(\beta = 1, \eta = 0)$	95.92	11.33	0.34	0.034
$(\beta = 1, \eta = 1)$	97.49	9.49	0.35	0.032

Table 5: Performance of FaIRL on Biographies dataset in different configurations involving the debiasing component. The best results are highlighted in **bold**.

metrics achieved by FaIRL in different configurations on Biographies dataset. We observe that removing debiasing component completely (configuration: $\beta = 0, \eta = 0$), results in drop in target accuracy as well as leakage of protected attribute, resulting in poor fairness metric scores. We believe the poor performance in target task occurs as the feature space doesn't remain compact due to the removal of debiasing component, which hinders incremental learning. We observe similar results with $(\beta = 0, \eta = 1)$ configuration, but the accuracy is slightly better due to the presence of debiasing component of \mathcal{X}_{old} , as it also helps in keeping the feature space compact. Only having the debiasing component for \mathcal{X}_{new} (configuration $\beta = 1, \eta = 0$), results in better performance both in terms of accuracy and fairness metrics, falling slightly short of the configuration $(\beta = 1, \eta = 1)$.

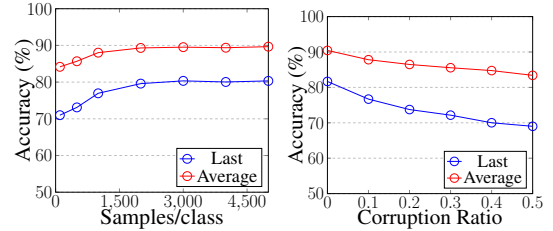


Figure 10: Performance of FaIRL on Biased MNIST (a) with varying samples per class; (b) at different label corruption ratios.

Sample Efficiency. In this experiment, we evaluate the sample efficiency of FaIRL by controlling the number of instances per class. We perform this experiment on Biased MNIST dataset ($p = 0.8$), where the number of instances per class is mostly uniform. In Figure 10(a), we report the average and final accuracy achieved by FaIRL. We observe that FaIRL is quite sample efficient achieving similar performance with 1000 samples/class (originally there were ~ 6000 samples/class). FaIRL achieves strong performance even with as small as

Method	$p = 0.8$		$p = 0.85$		$p = 0.9$		$p = 0.95$	
	DP	Gap _g ^{RMS}	DP	Gap _g ^{RMS}	DP	Gap _g ^{RMS}	DP	Gap _g ^{RMS}
LwF (Li and Hoiem, 2017)	0.19	0.046	0.29	0.124	0.56	0.230	1.57	0.548
Adversarial LwF	0.36	0.148	0.15	0.098	1.01	0.398	0.77	0.298
iCaRL (Rebuffi et al., 2017)	0.33	0.263	0.47	0.326	0.43	0.334	0.29	0.170
FaIRL (random)	0.13	0.047	0.12	0.067	0.18	0.087	0.50	0.237
FaIRL (prototype)	0.12	0.048	0.14	0.058	0.20	0.105	0.56	0.249
FaIRL (submod)	0.12	0.050	0.12	0.070	0.22	0.114	0.63	0.305

Table 6: Amortized Demographic Parity and Gap_g^{RMS} scores of incremental and joint learning systems on Biased MNIST dataset. FaIRL achieves the best performance among incremental learning baselines. Best results shown in **bold**.

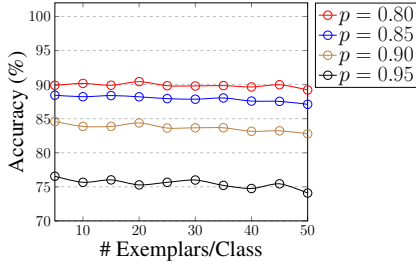


Figure 11: Accuracy with varying exemplar sizes.

100 samples/class.

Label Corruption. In this experiment, we evaluate the robustness of FaIRL by corrupting labels in the training data. Specifically, we corrupted varying fractions of target attribute labels in the training set and report the average and final performance. In Figure 10(b), we observe a graceful degradation in performance as the label corruption ratio increases. Even at high corruption ratios, we observe that FaIRL shows strong average performance, which showcases the robustness of our representation learning system.

Effect of exemplar size. We perform ablation experiments on Biased MNIST to investigate the effect of exemplar set size on FaIRL’s performance. In Figure 11, we observe that the average target accuracy almost remains constant with different exemplar sizes in all settings. This shows that FaIRL is robust to exemplar set size and can perform well with as small as 5 samples/class.

D Additional Results

Biased MNIST. We report the fairness metrics – average DP and Gap_g^{RMS} scores for incremental learning systems on Biased MNIST dataset in Table 6. We observe that FaIRL outperforms the baseline approaches in most settings except $p = 0.95$. In the setting with $p = 0.95$, iCaRL achieves

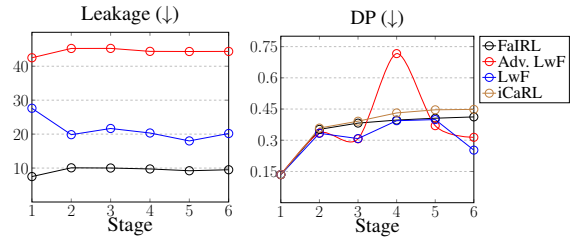


Figure 12: Evolution of gender leakage and Demographic parity across training stages on Biographies dataset.

the best score by a small margin which can be attributed to its relatively poor test accuracy.

Biography classification. We report the gender leakage and demographic parity of incremental learning systems across different training stages in Figure 12 (expected trends for the metrics are shown using \uparrow / \downarrow). Gender leakage is evaluated by probing the representations for protected attribute. We do not report the leakage for iCaRL as it performs prediction using nearest class estimator (NCE). In Figure 12(a), we observe that FaIRL leaks the least amount of information among the baselines. In Figure 12(b), we observe that FaIRL performs fairly well on demographic parity only falling short of LwF-based systems that suffer from catastrophic forgetting. FaIRL consistently outperforms iCaRL, which achieves a good performance on classification task.

E Broader Impacts and Limitations

Machine learning systems have revolutionized recommendations and decision-making in several applications like social media, over-the-top media industry etc. Over the years learning systems are found in critical applications like hiring, criminal recidivism etc. There are several positive benefits

of having data-driven fair machine learning systems in such systems. However, a major drawback of such systems is that they are trained offline using prior data, tested in a single domain, and then deployed in the wild. Often it is expensive to monitor and control decisions made by such systems. In recent years, a large body of works have focused on developing systems that are fair towards different demographic groups. However, the efficacy of these approaches are unknown when faced with unseen data. There is a need for having systems that can continually adapt to new data in the wild. We believe that our proposed problem of developing incrementally trained fair machine learning systems is a first step towards this goal. Incrementally trained fair systems would pave the way for having systems that drive decisions in the wild, and enable organizations to deploy them in critical applications.

Limitations. We present FaIRL, a novel fair representation learning system that can be trained in an incremental manner. One of the limitation of our system is that it relies on having protected attribute annotation to debias representations. Such annotations are expensive, and may not be accurate in all scenarios. For example, in our experiments we use only binary gender labels without considering other possible gender identities. Prior works have also shown that debiasing a system w.r.t a single protected attribute can sometimes make it biased towards other demographic groups. FaIRL relying on protected labels can also hinder learning of the target task, when the protected and target attributes are strongly correlated. Therefore, it is important for future systems to identify biased shortcuts used by a model, and prevent the system from using them for final predictions.

Negative Usage. We proposed FaIRL with the intention of achieving fairness using machine learning systems in the real-world. However, our approach can be misused if developers it to learn sensitive information instead of debiasing representations from it. In such cases, it easy to flag such systems using the fairness metrics discussed in Section 5.

We hope that our proposed task of incrementally learning fair systems would encourage others to develop more robust systems and help achieve fairness in the wild.